The 10th JFPS International Symposium on Fluid Power FUKUOKA 2017 Oct. 24-27, 2017 The Japan Fluid Power System Society

A STUDY OF A CYLINDRICAL TWO-STEP POLE TYPE ELECTRO-MAGNETIC ACTUATOR FOR CONTROLLING PROPORTIONAL HYDRAULIC VALVE (Examination of Basic Characteristics)

Hisao KONDO* and Yasunori WAKASAWA*

*Department of Mechanical Engineering, National Institute of Technology, Toyota College
2-1 Eisei-cho, Toyota, Aichi, 471-8525 Japan
(E-mail: hkondo@toyota-ct.ac.jp)

Abstract. In the previous report, a newly designed electro-magnetic proportional actuator composed of an armature and a stator with a cylindrical two-step pole to control oil hydraulic valve was suggested. In this actuator, two traction forces generated by the magnetic flux flow in the radial and the axial air gaps between the armature and the stator were added. These air gaps were arranged at two places in the magnetic circuit of the actuator, so the total of the traction forces became a large thrust force on the actuator. However, energy conversion process of this actuator was unclear in detail. In this study, the thermal characteristics of this actuator were examined with the thrust force characteristics. These characteristics are obtained by the result that the electrical energy supplied to the actuator is converted to the magnetic energy and thermal energy. Therefore, it is important to examine these characteristics for designing actuators.

Keywords: Fluid Power, Electro-Magnetic Proportional Valve, Valve Actuator, Two-Step Pole, Energy Conversion

INTRODUCTION

In the previous report [1], a newly designed electro-magnetic proportional actuator composed of an armature and a stator with a cylindrical two-step pole to control oil hydraulic valve was suggested. This actuator generates a large thrust force. The principal of generating force and the performance of the actuator were described in the report. All component shapes of this actuator were cylindrical so it was easy to manufacture. There are various types of conventional actuators for operating electro-magnetic control valves: proportional solenoids, force motors, torque motors and linear motors [2]. However these conventional actuators can not generate a large thrust force. One of the authors, with other researchers, designed a multi-step pole type electro-magnetic actuator, and constructed and examined it experimentally. Then the experimental results were reported [3]-[4]. This actuator can generate a large thrust force. However, the detail of the energy conversion process of the cylindrical two-step pole type and multi-step pole type actuators was unclear. In this study, the thermal characteristics of the cylindrical two-step pole type actuator were examined with the thrust force characteristics. These characteristics are obtained by the result that the electric energy supplied to the actuator is converted to the magnetic energy and thermal energy. After that, this magnetic energy is converted to mechanical energy and the actuators generate a thrust force. Therefore, it is important to examine these characteristics for designing actuators. Furthermore, in this experiment, the thrust force and electro-magnetic characteristics were examined in regards to the Pulse Width Modulation method used for driving the actuator.

STRUCTURE AND THRUST FORCE CHARACTERISTICS OF THE ACTUATOR

Figure 1 shows the structure of the actuator in this work. This actuator is composed of a stator, armature, winding guide, coil and pin. All of the component shapes are cylindrical. Figure 1 shows the axial cross sectional view. The stator shape is stepped at A and B, so the stator has rectangular edges beside the rectangular edges of the armature at these places. The armature can slide freely along the bore of the winding guide. Soft steel (SS400) is used for the material of the stator and the armature because this steel is easily obtained. In the actuator, the magnetic flux flow surrounds the coil when electric current flows through it. Then the magnetic fluxes ϕ_{a1}, ϕ_{a2}, ϕ_{r1}, ϕ_{r2} flow respectively across the axial and the radial air gaps between the stator and the armature at the edges of A and B. The magnetic flux flows ϕ_{r1} and ϕ_{r2} incline at $\alpha°$ as shown in Fig.1. The traction force F_a in the axial air gaps is generated by magnetic fluxes ϕ_{a1} and ϕ_{a2}, and the traction force F_r in the radial air gaps is generated by the magnetic fluxes ϕ_{r1} and ϕ_{r2}. The total force of these two forces becomes the

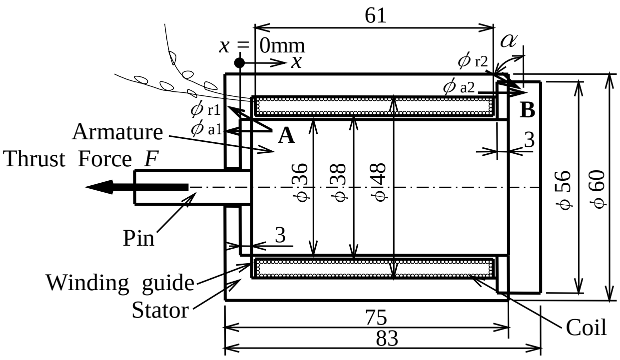

FIGURE 1. Structure of the actuator in this work

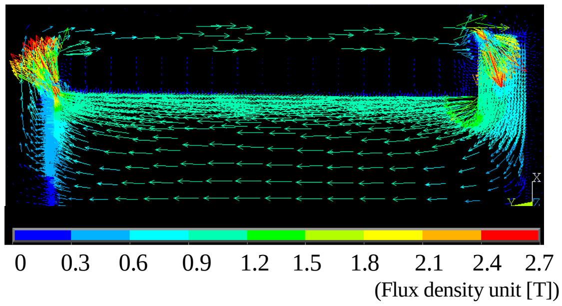

FIGURE 2. Magnetic vector diagram of the actuator (x = 2mm, NI = 1106AT)

thrust force of this actuator. In Fig.1, the armature position is indicated as x. When the end faces of the armature contact the end faces of the stator, the position x is defined as $x = 0$.

Figure 2 shows an analyzed magnetic vector diagram of the actuator. This figure is illustrated in the upper side half view of the section in Fig.1. The thrust force characteristics and magnetic flux flow were examined using magnetic field analysis, using software [5] that carries out the Finite Element Method Analysis. As shown in Fig.2, the magnetic fluxes flow as mentioned above. Furthermore, as shown in Fig.2, the magnetic fluxes density is high at the rectangular edges of the magnetic poles, and the density in the axial air gap between the stator and the armature is also higher than the density in other areas.

Figure 3 shows the thrust force characteristic curves of the actuator in Fig.1. The thrust force F_{add} curve is obtained by the addition of two traction forces, F_a and F_r. So, the test actuators, which generate these two traction forces separately, were made and examined to find the thrust force curve F_{add}. Additionally, this figure shows the comparison of the analyzed values and the experimental values of the thrust force F when the armature position x is varied. In these prototype actuators shown in Fig.1, magneto motive force NI (N: coil winding number, I: electric current of coil) is calculated based on the size of the coil winding guide. As a result, NI is 1106AT (Ampere Turn) at an electric power consumption of 15W, which is the same as a conventional proportional solenoid of the same size. The thrust force characteristics were examined at this magneto motive force. As shown in Fig.3, the thrust force curves of F_{add} and F agree well each other when x is larger than 1mm. The thrust force F becomes constant in the range of 1mm to 3mm of the armature position x in Fig.1. This range is used for the working stroke of the suggested proportional actuator in this study.

Figure 4 shows the relationship between the magneto motive force NI and the thrust force F on the condition that armature position x is fixed at 2mm. As shown in Fig.4, the thrust force F is in proportion to the magneto motive force NI in the range of 250AT to 1800AT. When magneto motive force NI equals 1106AT at an electric power consumption of 15W, the thrust force F is in the proportional area in Fig.4.

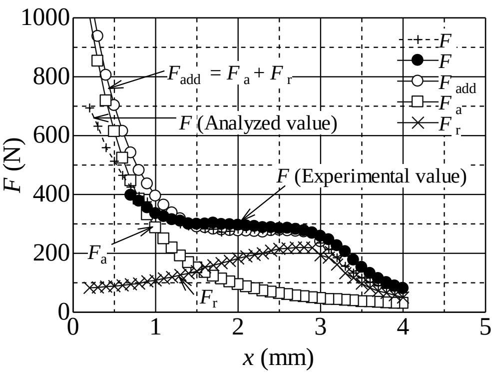

FIGURE 3. Relationship between the thrust force F and the traction forces F_a, F_r

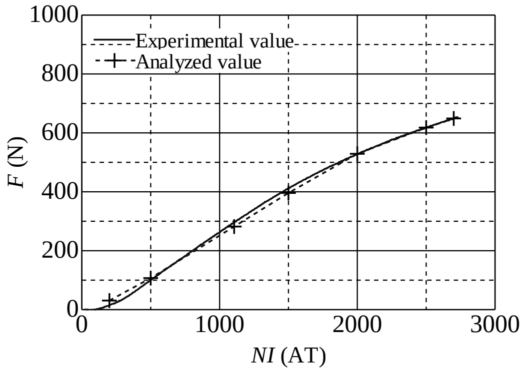

FIGURE 4. Relationship between NI and F (x=2.0mm)

BASIC CHARACTERISTICS OF THE ACTUATOR

The electro-magnetic actuators perform mechanical work by using the supplied electric energy, which is converted to magnetic energy and then converted to mechanical energy in the actuator. In this energy conversion process, a part of the supplied electric energy is converted to Joule heat, which does not contribute to the mechanical work. The basic characteristics of the energy conversion are described as follows:

The equivalent electric circuit of the electro-magnetic proportional actuator is considered as connecting coil inductance L and coil resistance R serially. When the voltage V is supplied to the coil of the actuator from a power supply, the electric current equation becomes as follows:

$$V = L\frac{di}{dt} + Ri \tag{1}$$

where i is electric current and t is time. In Eq. (1), when both side are multiplied by i and integrated at the time from the instance of applying the voltage V to the electric current i becoming I, the energy equation becomes as follows [6]:

$$\int_{i=0}^{i=I} Vidt = \int_{i=0}^{i=I} Lidi + \int_{i=0}^{i=I} Ri^2 dt \tag{2}$$

In Eq. (2), the left side indicates the total energy supplied from the electric supply, the first term on the right side indicates the magnetic energy stored in the magnetic circuit of the actuator, and second term on the right side indicates the Joule heat in the electric circuit which is lost by heat transfer to the outside of the actuator. Furthermore, when the electric current i in the electric circuit changes from zero to I, and the magnetic flux ϕ in the magnetic circuit of the actuator changes from zero to ϕ_1, then the first term on the right side in Eq. (2) can be written as follows [7]:

$$\int_{i=0}^{i=I} Lidt = \int_{\phi=0}^{\phi=\phi_1} Nid\phi \tag{3}$$

The right side in Eq. (3) indicates the magnetic energy in the magnetic circuit of the actuator.
In general, the magnetization curve of the electro-magnetic actuator is as shown in Fig.5. In Fig.5, when the armature position x is moved from x_1 to $x_1+\Delta x$ while electric current i through the coil is kept at a constant value I, the magnetic flux ϕ increases from point a to point b. At this time, the magnetic energy in the actuator is converted to mechanical energy as follows [7]:

$$F \cdot \Delta x = Area \text{ oabo} \tag{4}$$

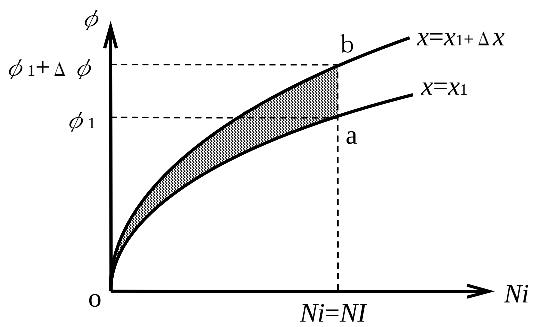

FIGURE 5. Magnetization curve of the actuator

where F denotes the thrust force generated on the actuator, and Δx denotes a very small displacement of the armature. According to Eq. (4), to obtain a large thrust force from the electro-magnetic actuators, it is necessary to magnify the area of the range of the oblique line in Fig.5; in other words, to magnify the changes in the amount of the magnetic energy when the armature moves Δx.
Next, when the coil of the electro-magnetic actuator is energized continuously, the coil is heated by Joule heat as shown the second term on the right side in Eq. (2). A part of this heat is accumulated into the actuator, and the other part is lost by heat transfer to the outside of the actuator. So, the thermal equilibrium equation of the electro-magnetic actuator in a very small lapse of time Δt is written as follows [6]:

$$mc\Delta\theta + hA(\theta - \theta_0)\Delta t = W\Delta t \tag{5}$$

where $\Delta\theta$ is the rising temperature, m is the mass, c is the specific heat, h is the heat transfer coefficient, A is the surface area, W is the Joule heat of the coil, θ is the temperature of the actuator and θ_0 is the room temperature. In Eq. (5), the first term on the left side indicates the accumulated amount of thermal energy into the actuator, the second term indicates the heat transfer amount to the outside of the actuator, and the right side indicates the Joule heat of the coil in the actuator which is equal to the second term on the right side in Eq. (2). When Eq. (5) is rewritten as a differential equation and is solved in relation to the temperature θ, the equation of the rising temperature of the actuator is obtained as follows [6]:

$$\theta = \theta_0 + \frac{W}{hA}(1 - e^{-\frac{hA}{mc}t}) = \theta_0 + \theta_f (1 - e^{-\frac{t}{\tau}}) \tag{6}$$

where θ_f is the saturated temperature after the rising temperature which is equal to W/hA, and τ is the thermal time constant at the rising temperature which is equal to mc/hA. Moreover, when the coil is energized continuously, the relationship between the temperature θ and the resistance R of the coil of copper is as follows [6]:

$$R = \frac{234.5 + \theta}{234.5 + \theta_0} R_0 \tag{7}$$

where R_0 is the coil resistance at the room temperature. According to Eq. (7), the coil resistance R becomes higher when the coil temperature θ is raised higher than the room temperature. Here, it is necessary to note that the lost energy becomes greater because the Joule heat of the actuator becomes greater if the coil current is kept constant.

EXPERIMENTAL RESULTS OF THE ELECTRO-MAGNETIC CONVERSION CHARACTERISTICS

Figure 6 shows the experimental results of the relationship between the magneto motive force *NI* and the magnetic flux ϕ in the actuator as shown in Fig.1. In these experiments, a couple of coils of 360+360 turns are used. One coil is used for magnetizing the actuator, and the other one is used for the search coil. So, this search coil detects the magnetic flux, which flows in the armature in the axis direction. As shown in Fig.6, the magnetizing curves change with the armature position x. The rectangular edges of the magnetic poles of the stator and the armature begin to overlap each other when x = 3mm as shown in Fig.1. And then, when x becomes smaller than 3mm, the overlap of these poles becomes greater. Furthermore, the axial air gaps between the faces of the stator and the armature become smaller, so the magnetic flux flows easily across the axial and radial air gaps. Therefore, as shown in Fig.6, the magnetizing curve moves upward when x becomes smaller. As shown in Fig.5, the larger the change of the magnetic energy when the armature moves Δx, the more mechanical energy is created, and the larger the thrust force F on the actuator becomes.

The key feature of the electro-magnetic proportional actuator in this study is having a flat coil in the actuator. Therefore the cross sectional area of the magnetic path in the stator and the armature is larger than that of conventional proportional solenoids, as shown in Fig.1. In addition, the magnetic poles, which are opposed between the stator and the armature, are arranged serially at two places in the magnetic circuit of the actuator. So the amount of magnetic flux change caused by varying the armature position becomes larger, and then a larger thrust force can be generated.

Figure 7 shows the relationship between the magneto motive force *NI* and the thrust force F, which is converted from the magnetic energy shown in Fig.6 using Eqs. (3) and (4). In Fig.7, the dotted line indicates the converted

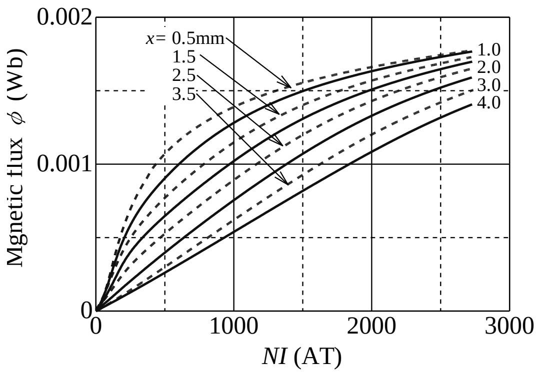

FIGURE 6. Relationship between *NI* and ϕ

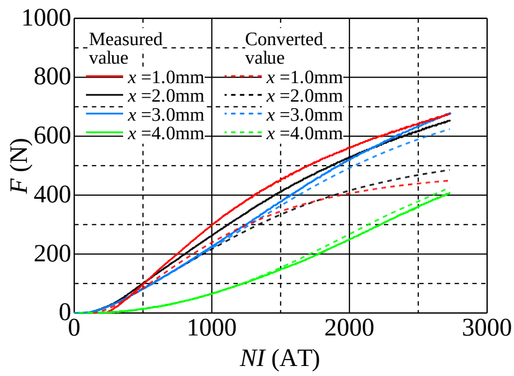

FIGURE 7. Comparison of the thrust force F

4

thrust force, and the solid line indicates the measured thrust force using a load cell. As shown in Fig.7, the measured values and converted values of the thrust force F agree well each other when x is larger than 3mm. When x is less than 2mm, it means that in the overlapped position of the magnetic poles of the stator and the armature, the magnetic flux flows between the magnetic poles of the stator and the armature incline at the angle α° as shown in Figs.1 and 2. When the shapes of the opposed end faces of the stator and the armature in the axial direction are cones, thrust force F becomes $F=F_0/\cos^2\alpha$ [8]. Where F_0 is the thrust force when the end face shapes are flat, and the amount of the magnetic flux flow of the armature in the axial direction is the same in the case of both the cone shaped and flat shaped end faces. In Fig.7, when x is less than 2mm, the measured values of the thrust force F is 1.3 times greater than the values of F_0, so F/F_0=1.3. Using above mentioned equation, α is found to be 28.7° . The angle of the magnetic flow between the rectangular magnetic poles of the stator and the armature in Fig.2 is nearly equal to this angle α. Therefore, the thrust force of the measured values and converted values do not agree each other in Fig.7 when x is less than 2mm. However, in consideration of these, it becomes clear that the differing amount of magnetic energy caused by varying the armature position x was converted to the thrust force F completely in the studied actuator.

EXPERIMENTAL RESULTS OF THE THERMAL CHARACTERISTICS

To examine the thermal characteristics of the studied actuator, the actuators having cylindrical shaped stator in Fig.8 (a) and square shaped one with fins in Fig.8 (b) were used. The outer dimension d of these stators are 60mm for the diameter of the cylindrical shaped stator (a), and for the sides of the square shaped stator (b) in the experimental actuator.

Figure 9 shows the experimental results of the rising coil temperature curves of the actuators having the different shaped stators in Fig.8 (a) and (b), resulting in a varying electric power consumption W_{20} at the room temperature 20℃, when the coil is energized continuously by constant electric current. In Fig.9, the solid line indicates measured curves, and the dotted line indicates the fitting approximated curves, which determine the rising coil temperature curves until the saturation temperature is reached. These approximated curves can determine the saturation temperature θ_f in Eq. (6). As shown in Fig.9, saturated temperature θ_f becomes higher as the electric power consumption W_{20} becomes greater in the both actuators having cylindrical shaped stator and square shaped stator with fins. When the rising coil temperature curves of the actuators with differently shaped stator are compared with each other at the same level of electric power consumption, the time it takes to

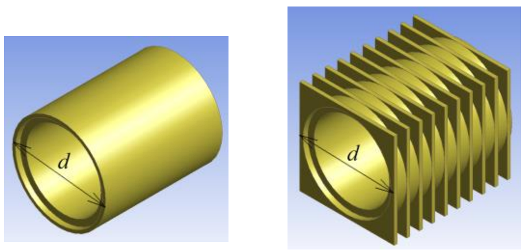

(a) Cylindrical shape (b) Square shape with fins

FIGURE 8. Stator shapes in this work

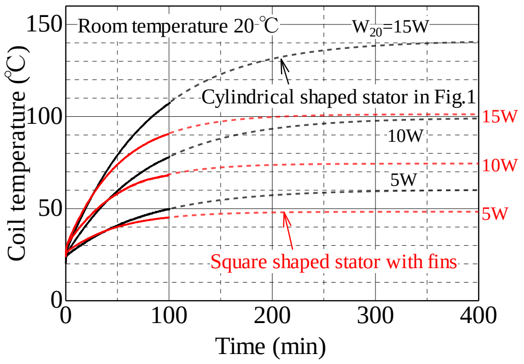

FIGURE 9. Experimental results of the rise in coil temperature

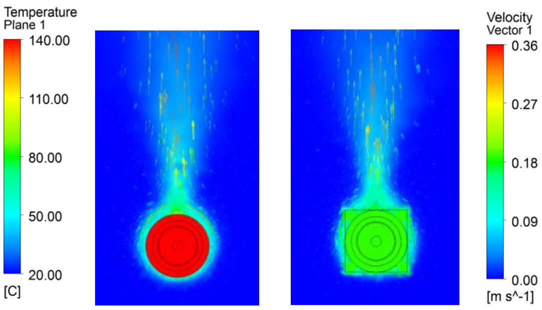

(a) Cylindrical shape (b) Square shape with fins

FIGURE 10. Analyzed diagrams (W_{20}=15W)

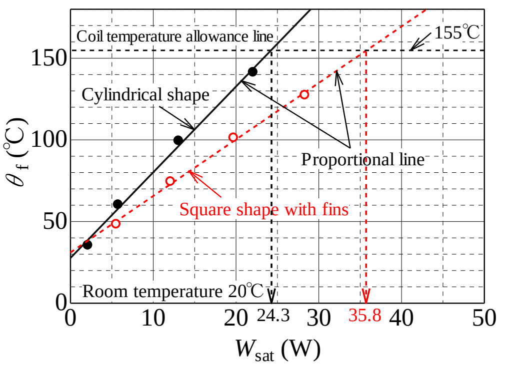

FIGURE 11. Relationship between W_{sat} and θ_f

reach the saturated temperature in the actuator having a square shaped stator with fins is shorter, and the saturated temperature in this actuator is lower than those in the actuator having a cylindrical shaped stator. Because, in Eq. (6), the surface area A of the actuator having the square shaped stator with fins is larger than that of the actuator having the cylindrical shaped stator.

Figure 10 shows the analyzed temperature contour and the velocity vector diagrams of the actuator at the saturated temperature. The analyzed diagrams in Fig.10 were created by using thermal fluid analysis, using Finite Element Method Analysis software [9]. As shown in Fig.10, the analyzed saturated temperature almost agrees with the measured temperature in Fig.9. And it becomes clear that the heat transfer of this actuator is caused by natural convection as shown in Fig.10.

Figure 11 shows the experimental results of the relationship between the electric power consumption W_{sat} at saturated temperature and the saturated temperature θ_f. As shown in Eq. (6), the saturated temperature θ_f is equal to W_{sat}/hA, so the saturated temperature θ_f is proportional to the electric power consumption W_{sat} in Fig.11. The coil which is used in the studied actuator has a temperature allowance of 155℃. The cross points between the coil temperature allowance line and the proportional lines are found in Fig.11. The limit of the usable electric current of this actuator can be determined by the electric power consumption at these cross points. We can see that the actuators having cylindrical shaped and square shaped stators can be used up to W_{sat} values of 24.3W and 35.8W respectively. From Eqs. (6), (7) and the Joule heat equation $W=RI^2$, the electric power consumption W_{20} at the room temperature 20℃ can be calculated. As a result, the W_{sat} values of 24.3W and 35.8W becomes W_{20} values of 15.8W and 23.4W respectively. Using the experimental results of the thrust force as shown in Fig.4, maximum thrust forces F values of 306N and 378N at W_{20} values of 15.8W and 23.4W are found respectively.

EXPERIMENTAL RESULTS OF PWM DRIVING CHARACTERISTICS

In general, electro-magnetic actuators are operated by Pulse Width Modulation (PWM) driving, which has high efficiency. In the case of the PWM voltage driving the electro-magnetic actuator, it is necessary to examine the fluctuations of the electric current of the coil, the magnetic flux and the thrust force. To examine the magnetic flux in the prototype actuator, a couple of coils of 360+360 turns were used as shown in Fig.6.

Figure 12 shows the square waveform characteristics when the modulated frequency f is 1Hz, the duty ratio of PWM is 50% and these are fixed values. As shown in Fig.12, the current I, the search coil voltage V_ϕ and the thrust force F fluctuate from zero to their maximum values in relation to the amount of the supply voltage V. Figure 13 shows the changes of the magnetic flux ϕ and the thrust force F when the electric current of the coil

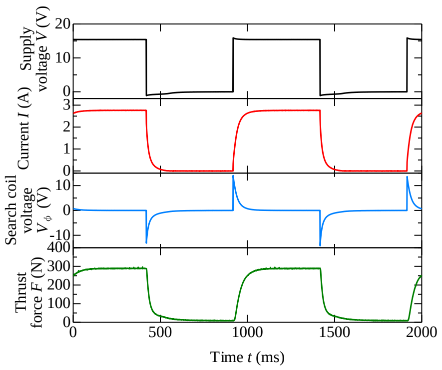

FIGURE 12. Square waveform characteristics (f=1Hz, duty ratio=50%)

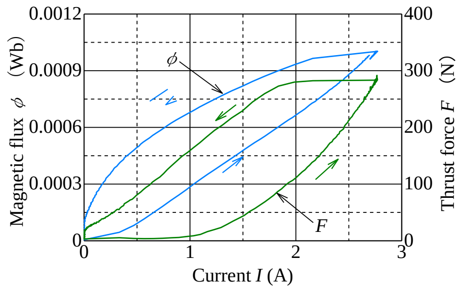

FIGURE 13. Hysteresis curves in Fig.12

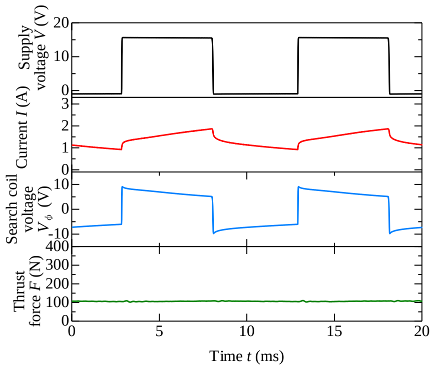

FIGURE 14. Square waveform characteristics (f=100Hz, duty ratio=50%)

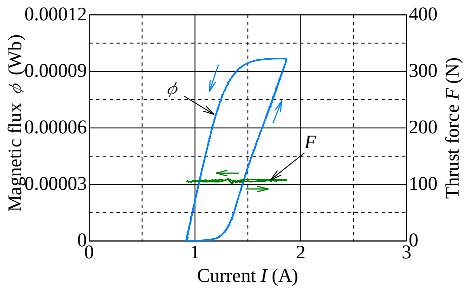

FIGURE 15. Hysteresis curves in Fig.14

increases and decreases from zero to its maximum value and back again in Fig.12. As shown in Fig.13, hysteresis of the magnetic flux ϕ and thrust force F in this actuator are caused by increasing and decreasing the electric current. And the thrust force F is delayed more than the magnetic flux ϕ in relation to the change of the electric current I. Therefore, the hysteresis of the thrust force is larger than that of the magnetic flux.

Figure 14 shows the square waveform characteristics when f and the duty ratio have fixed values of 100Hz and 50% respectively. As shown in Fig.14, when the modulated frequency f of the PWM is relatively high, the fluctuations of current I, the search coil voltage V_ϕ and the thrust force F become less compared with value of f in Fig.12, because the coil inductance is relatively large and the rise of the coil current is not fast enough to keep up with the changes in the supplied voltage. Figure 15 shows the changes of the magnetic flux ϕ and the thrust force F when the electric current changes as in Fig.14. As shown in Fig.15, the fluctuation width of the magnetic flux ϕ becomes one tenth of the amount of ϕ at the modulated frequency f of 1Hz. However, the fluctuation width of the thrust force F becomes nearly zero. The reason for these changes is that the delay of the change of the thrust force F becomes larger in relation to the change of the magnetic flux ϕ when the modulated frequency becomes higher. Therefore, if the modulated frequency f of PWM is chosen properly, the fluctuation of the thrust force F could be small to nearly zero.

Figure 16 shows the relationship between the modulated frequency f of PWM, the fluctuation width (Max-Min) of the current I and the thrust force F. As shown in Fig.16, when the frequency f is higher than 100Hz, fluctuation width of the current I becomes small and the width of the thrust force F becomes nearly zero. However, when the modulated frequency is very high, for example 1000Hz, the waveform of the current I becomes very irregular.

Next, Table 1 shows the relationship between the supplied electric energy, the magnetic energy, and the Joule heat energy that are found in the experimental values in Figs. 12 and 14 using Eqs. (2) and (3). As shown in Table 1, when the modulated frequency f is low, for example 1Hz, Joule heat energy is much greater than the magnetic energy converted from the supplied electric energy. When f is high, for example 100Hz, the Joule heat energy becomes closer to the magnetic energy. As mentioned above, the Joule energy of the actuator is wasted as the heat of the actuator itself and heat transfer to the outside of the actuator. Magnetic energy is converted to mechanical energy, and the actuator generates the thrust force. Therefore, it is also important to examine the relationship to obtain more magnetic energy from the supplied electric energy when designing electro-magnetic actuators.

In the next experiment, as shown in Fig.17, the duty ratio is varied continuously from 1% to 100%, and then the duty ratio is decreased from 100% to 1% by 1% each time. In consideration of the transient response of the current due to change in the supplied voltage, the duty ratio is varied after using the same ratio three times. This experimental results are shown in Fig.18. As shown in Fig.18, when the modulated frequency of the PWM is 100Hz, the current I and the magnetic flux ϕ change slowly with small fluctuations following the change of the duty ratio of the PWM. However, we can see that the fluctuations of the thrust force F is smaller than that of the current I and the magnetic flux ϕ in the above mentioned Figs.14 and 15.

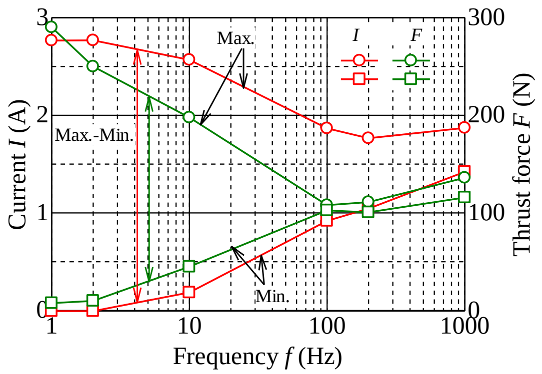

FIGURE 16. Fluctuation width of the current and the thrust force

TABLE 1. Relationship between each energy

Modulated Frequency f (Hz)	**Supplied Electric energy** $\int VIdt$ (J)	**Magnetic Energy** $\int Nid\phi$ (J)	**Joule Heat** $\int RI^2dt$ (J)
1	20.2	1.02	19.0
100	0.126	0.0539	0.0707

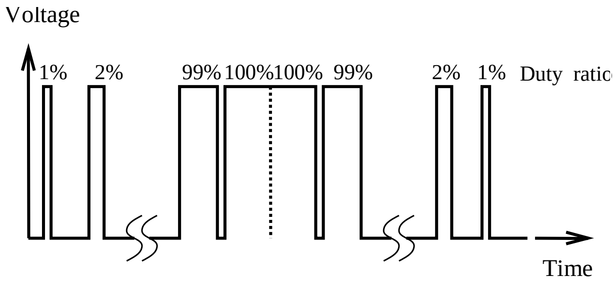

FIGURE 17. Variable diagram of the duty ratio

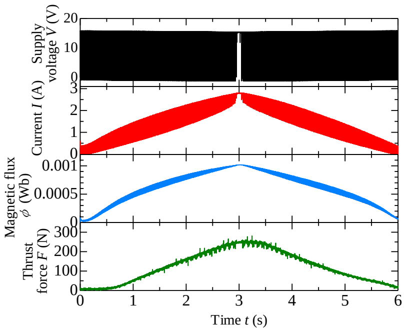

FIGURE 18. PWM driving characteristics (f=100Hz, duty ratio=variable)

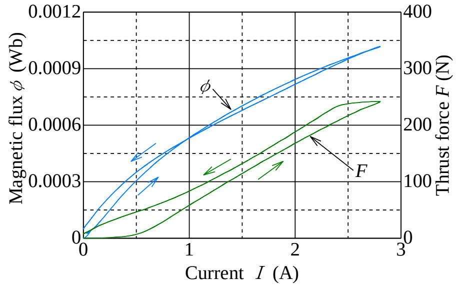

FIGURE 19. Hysteresis curves in Fig.18

To examine the hysteresis of the magnetic flux ϕ and the thrust force F for varying the current I in Fig.18, small fluctuations of each waveforms are removed using Low Pass Filter (LPF) processing. Fig.19 shows the hysteresis curves of ϕ and F when varying I after LPF processing. As shown in Fig.19, the hysteresis of the magnetic flux ϕ is very small, but the hysteresis of the thrust force F is relatively large. Especially, when the current I is less than 1A (magneto motive force NI is 360AT) and around 2.8A (NI is 1000AT), the hysteresis of the thrust force F is large. Except for these ranges, the thrust force F is almost proportional to the electric current I, and the hysteresis of F is less than 10%. The magnetic material of this prototype actuator has relatively large magnetic hysteresis. So the hysteresis of the thrust force F may decrease if using a magnetic material having low magnetic hysteresis.

CONCLUSIONS

In this study, the basic characteristics of the cylindrical two-step pole type electro-magnetic proportional actuator suggested in the previous report, which are the thrust force, the electro-magnetic conversion, thermal and the PWM driving characteristics, were examined experimentally. In the results, it became clear that the suggested actuator can generate a large thrust force, since the change in magnetic energy when varying the armature position was large. In this actuator, the rise in coil temperature was examined when the actuator was energized continuously and it was clarified how the experimental result of these thermal characteristics are useful for designing the actuator. Furthermore, it was confirmed that the supplied energy was converted to magnetic energy and Joule heat completely. The PWM driving characteristics were examined, and it became clear that the fluctuation of the thrust force became nearly zero when choosing a properly modulated frequency, having the thrust force proportional to the electric current, having the hysteresis of the thrust force less than 10%. When designing the electro-magnetic actuators, it may be need to examine the processes of converting of electric, magnetic, mechanical and thermal energy as reported in this study.

ACKNOWLEDGMENTS

The authors would like to express their appreciation to students of National Institute of Technology, Toyota College.

REFERENCES

1. KONDO, H., TAKEUCHI, R., WAKASAWA, Y.: A Study of a Cylindrical Two-Step Pole Type Electro-Magnetic Proportional Actuator, JFPS International Journal of Fluid Power System, 2016, Vol.9, No.1, pp.1-10
2. BACKE, W. : Grundlagen und Entwicklungstendenzen in der Ventiltechnik, O+P, Vol.34, No.7, 1990, pp.496-505
3. KONDO, H., HIBI, A.: A Study of a Multi-step Pole Type Electro-magnetic Actuator for Controlling Proportional Hydraulic Valve, JFPS International Journal of Fluid Power System, 2009, Vol.2, No.2, pp.9-14
4. KONDO, H., KURATA, Y.: A Study of a Multi-step Pole Type Electro-magnetic Actuator for Controlling Proportional Hydraulic Valve (Magnetic Flux Flow in the Actuator), JFPS International Journal of Fluid Power System, 2015, Vol.8, No.2, pp.82-89
5. CYBERNET SYSTEMS Co., Ltd.: ANSYS Magnetic Field Analysis Seminar Note, (in Japanese), 2011
6. NAKATA, T., ITO, S., KAWASE, Y.: Design and application of AC/DC Electromagnets using FEM, Morikita Publishing Co., Ltd., (in Japanese), 1991, pp.63-70
7. MIYAIRI, S.: Electro-mechanical energy conversion, Maruzen Co., Ltd., (in Japanese), 1976, pp.3-9
8. MOGI, A.: Magnetic circuit, Kyoritsu Publishing Co., Ltd., (in Japanese), 1964, pp.173-174
9. CYBERNET SYSTEMS Co., Ltd.: ANSYS CFX Basic Seminar, (in Japanese), 2011